In: Proceedings of the ANTEC 2013 Conference; 2013

FABRICATION AND CHARACTERIZATION OF POLYVINYL ALCOHOL (PVA)/NANOFIBRILLATED CELLULOSE (NFC) FILAMENTS

Jun Peng[1, 2], Yottha Srithep[1], Ronald Sabo[3], Srikanth Pilla[1], Xiang-Fang Peng[2], Lih-Sheng Turng[1], Craig Clemons[3*]*
[1]Polymer Engineering Center, University of Wisconsin-Madison, Madison, Wisconsin 53706, USA
[2]South China University of Technology, Guangzhou 510640, China
[3]Forest Products laboratory, USDA Forest Service, Madison, Wisconsin, 53726, USA

Abstract

This paper presents a new process to fabricate single polyvinyl alcohol (PVA)/nanofibrillated cellulose (NFC) filaments and measures their tensile properties at various NFC ratios (0.5 to 3 wt %). The fabrication process generally contains four steps: (1) NFC isolation, (2) preparation of the PVA/NFC solution, (3) gel spinning and drying, and (4) filament stretching. The ultimate strength of PVA/NFC increased by almost 2 times compared with stretched neat PVA filaments. In order to ensure that the NFC fibers dispersed well in the PVA solution, high shear processing was employed. To study the possible degradation of PVA caused by high shear, a parallel plate rheometer was used to investigate the viscosity of the PVA/NFC solutions. The PVA crystal orientation in the PVA/NFC filaments was characterized by wide angle x-ray diffraction (WAXD).

Introduction

Nanoscale cellulose reinforcing fillers possess attractive mechanical properties, which depend on crystal structure, crystallinity, anisotropy, defects, and separation approaches [1]. Several mechanical approaches have been employed to isolate cellulose fibrils from wood or plant fibers, such as refining [2], homogenizing [3], cryocrushing [4], high intensity ultrasonic treatment [5], and using a microfluidizer. Nanofibrilated cellulose (NFC) are cellulose fibrils obtained by mechanical isolation processes, whereas cellulose nanocrystals (CNC) are produced by acid hydrolysis extraction or enzymatic hydrolysis. NFC contains both amorphous and crystalline regions and a high aspect ratio (4 to 20 nm in width, 500 to 2000 nm in length) [1]. Iwamoto et al. prepared nanofibrillated cellulose fibers by TEMPO-mediated oxidation and achieved a tensile strength of 321 MPa [6]. Walther et al. reported that wet spun NFC fibers possessed a tensile strength of 275 MPa [7]. In a study by Sehaqui et al., the effect of NFC orientation on the tensile properties was investigated. The maximum tensile strength obtained was 400 MPa [8].

Polyvinyl alcohol (PVA) resin is water soluble, biodegradable, and biocompatible. Therefore, PVA-based fibers have been broadly investigated for tissue scaffolding, filtration materials, membranes, drug release, and so on [9]. To improve the mechanical properties of the PVA matrix, some nanoscale fillers like carbon nanotubes [10], clay [11], and cellulose nanofibrils were used as reinforcing fillers. Favier et al. was the first to use CNC as a reinforcing filler [12]. Uddin et al. produced wet spun fibers from a PVA/CNC solution, followed by hot drawing to enhance the tensile properties. With CNC reinforcing fillers, the ultimate tensile strength increased 20% as compared to neat PVA fibers [13]. Peresin et al. produced PVA/NFC nanofiber mats using the electrospinning process and found that nanofiber mats had a higher storage modulus when CNC fillers were present [14].

In this study, NFC was employed as the reinforcing filler to improve the PVA filament's tensile properties. The ultimate tensile strength and strain-at-break were characterized by filament tensile testing. PVA crystal orientation was quantified based on the wide angle X-ray diffraction (WAXD) pattern. While high shear is beneficial to maintaining good NFC dispersion in viscous PVA solutions, a strong shear stress may lead to a reduction in PVA's molecular weight. Potential material degradation due to molecular weight reduction was indirectly characterized by rheometric viscosity data.

Experimental Procedure

Materials and Processing Devices

A 99% hydrolyzed commercial-grade polyvinyl alcohol (PVA) from Sigma-Aldrich with a weight-average molecular weight of 85,000 to 124,000 was used in this study. A microfluidizer processor (M-110EH-30, Microfluidics) was employed to generate high shear for better NFC dispersion in both the NFC water solution and the PVA/NFC solutions. The microfluidizer had two microchannels with diameters of 200 and 87 μm, respectively. A commercially available fiber drawing device (DSM Xplore Fiber Spin Line) was used to stretch the filaments. The processing temperature was 200ºC and the draw ratio was kept constant at 5.

Testing Techniques

Transmission Electron Microscopy (TEM)

The NFC structure and dimensions were investigated by TEM. A drop of NFC solution (0.5 wt% in water) was deposited on the TEM copper grid and dried. The sample grids were observed by a JEOL JEM-2100 at an accelerating voltage of 80 kV.

Scanning Electron Microscopy (SEM)

The PVA/NFC filament cross-sections were analyzed by a scanning electron microscope (SEM; JCM-5000, JEOL, Japan) at an accelerating voltage of 10 kV.

* Corresponding Author: turng@engr.wisc.edu and cclemons@fs.fed.us

Viscosity

The rheometric properties were tested with a parallel-plate rheometer (TA EX2000). Two test modes were used: a steady-state shear mode at room temperature with a shear rate ranging from 0.1 to 400 s^{-1}, and a temperature scanning mode with a temperature range of 20 to 70ºC.

Wide-Angle X-ray Diffraction (WAXD)

An X-ray diffraction pattern was characterized by a diffractometer (Bruker/Siemens Hi Star 2D) with a mono-chromatic CuK (alpha) point source at 40 kV and 20 mA.

The degree of PVA crystal orientation, π, is defined as [13]

$$\pi=(180-H^{o})/180 \qquad (1)$$

where H^{o} is the half-width of the azimuthal intensity distribution curve along the Debye–Scherrer ring.

Tensile Testing

Due to the significant effects of temperature and the relative humidity on the physical properties of the filaments, all of the filament samples were stored at 23 ºC and 50% relative humidity for a week prior to testing. Tensile properties were measured at the same conditions using a tensile testing machine (Instron) with a 100 N load cell, a gauge length of 2.54 mm, and an extension rate of 0.254 mm/min following the ASTM D3379-75 standard. The experimental results were evaluated as an average of at least 6 measurements.

The PVA/NFC Filament Fabrication Process

As mentioned above, the fabrication process generally contains four steps: (1) NFC isolation (2) preparation of the PVA/NFC solution with good NFC dispersion, (3) gel spinning and filament drying, and (4) filament stretching at a constant draw ratio.

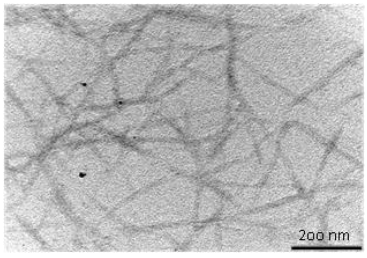

Figure 1. TEM image of TEMPO-oxidized cellulose with a concentration of 0.5 wt %.

The NFC isolation process followed Satio's approach [21]. Namely, a commercial hardwood bleached kraft pulp was oxidized by a 2, 2, 6, 6-tetramethyl-piperidine-1-oxyl radical (TEMPO)-mediated system. Then, 0.1 M HCl and 0.5 M NaOH were added to adjust the pH to 10. The TEMPO-oxidized rough cellulose first passed through a mechanical refiner, then a centrifuge to separate the coarse cellulose fibers. To further improve NFC dispersion in water, the NFC solution was forced through two microchannels (200 and 87 μm) of the microfluidizer processor. In the end, a 0.5 wt% NFC aqueous solution was produced. Figure 1 shows the TEM image of dried NFC fibers on a TEM copper grid depicting the uniform NFC dispersion and the nanofiber dimensions. In particular, the NFC exhibited a network structure with fibrils nano-scale in diameter and micro-scale in length.

To prepare PVA/NFC solutions, PVA powder was first dissolved in deionized (DI) water at 90 ºC while stirring for 30 mins. Next, NFC was added to the PVA solution to form the compositions shown in Table 1. Films casted from the PVA/NFC solutions were transparent, but the film surface was not flat due to non-uniform shrinkage. To improve NFC dispersion, the PVA/NFC solutions were forced through the microchannels of the microfluidizer three times. Afterwards, the solutions appeared transparent, suggesting uniform dispersion. In addition, their cast films were flat, and had constant thickness.

Table 1. PVA and NFC concentrations of PVA/ NFC solutions for gel spinning and in solid PVA/NFC filaments.

Sample	Solu. Concentration (wt%)		Solid Fiber Filament (%)	
	PVA	NFC	NFC/PVA ratio	NFC concentration
PVA/NFC3%	13.00	0.39	3.00	2.91
PVA/NFC2%	13.00	0.26	2.00	1.96
PVA/NFC1%	13.00	0.13	1.00	0.99
PVA/NFC0.5%	13.00	0.07	0.50	0.50
Pure Pva	13.00	N/A	N/A	N/A

To further investigate NFC dispersion, the viscosity of the solutions as a function of shear rate was determined using a parallel-plate rheometer (cf. Fig. 2). The reduction in viscosity of the pure PVA solution after treatment by the microfluidizer suggested that the high shear in the microfluidizer may have degraded the molecular weight of the PVA. On the other hand, the viscosity of the PVA/NFC solutions increased with increasing NFC content, suggesting a higher degree of PVA/NFC inter-action.

Filaments were prepared in a manner similar to Uddin et al [insert ref]. The PVA/NFC solutions were spun into cold ethanol (-20ºC) with a syringe pump. A 30 ml syringe with a 19 gauge (0.686 mm inner diameter) needle was used. The volumetric flow rate was set at 0.38 ml/min and the air gap between the needle tip and the ethanol surface was 1 to 2 mm. The apparent wall shear rate of the solution passing through the needle was estimated to be around 200 s^{-1}.

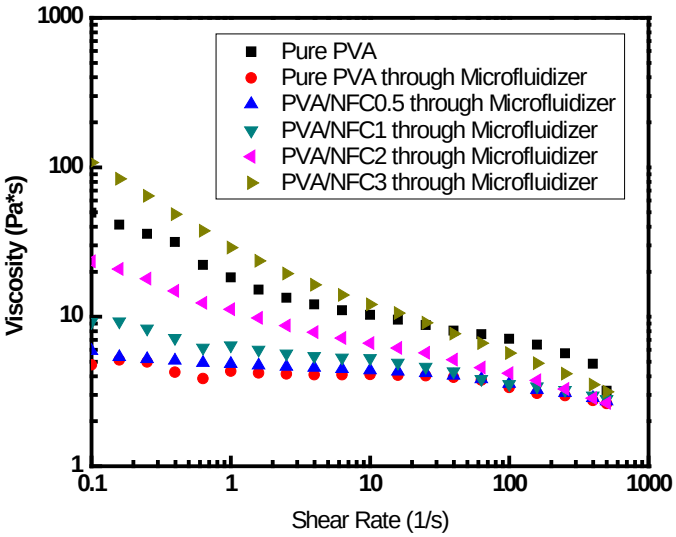

Figure 2. The viscosity curves of pure PVA and PVA/ NFC solutions with respect to shear rate.

Before being drawn, all of the wet spun PVA/NFC filaments were dried in ethanol for 48 hours, were air-dried , and then oven-dried at 90 ºC for 4 hours to remove the ethanol. All of the PVA/NFC filaments were stretched at 200 ºC with a draw ratio of 5. To calculate tensile strength, Table 2 tabulates the cross-section areas of the various filaments. The cross-section areas were estimated from the filament weight (24 in long) divided by the length and the density.

Table 2. PVA and PVA/NFC filament cross-section areas.

	Cross-section areas (10^{-4} cm^2)
Pure PVA	1.13
PVA/NFC0.5	1.35
PVA/NFC1	1.35
PVA/NFC2	1.38
PVA/NFC3	1.48

Results and Discussion

The representative stress–strain curves of the PVA and PVA/NFC nanocomposite filaments are plotted in Figure 3, while Figures 4 and 5 show the values of the ultimate tensile strength and strain-at-break, respectively

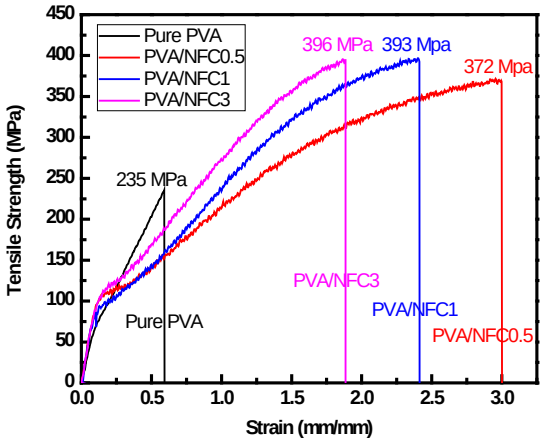

Figure 3. The mechanical properties of pure PVA and PVA/NFC filaments. The numbers 0.5, 1, and 3 refer to the NFC content in the PVA matrix.

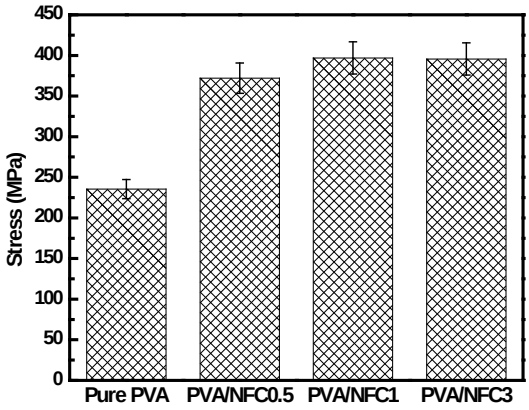

Figure 4. Ultimate tensile strength of pure PVA and PVA/ NFC filaments with different NFC contents.

PVA/NFC5 exhibited the maximum strength at 396 MPa, while PVA/ NFC0.5 achieved the maximum strain-at-break of all of the samples tested. Due to the network structure of NFC, which contains both crystalline and amorphous phases, NFC was able to improve both the tensile strength and strain-at-break of the PVA. With further additions of NFC, the strain at break decreased, likely as a result of NFC agglomeration and small voids caused by the relatively high NFC content.

PVA crystal orientation was shown to have a positive effect on the tensile properties of PVA/NFC filaments. The X-ray diffractograms, which are shown in Fig. 6, exhibit patterns for undrawn pure PVA filaments (referred to as DR=1), drawn pure PVA with DR=5, and PVA/NFC3 with DR=5. Reflections due to NFC are not able to be seen because of the low level of addition. Ring patterns were found on the reference undrawn pure PVA filaments, which correspond to a random PVA crystal distribution, as shown in Fig 6 (a). When drawn, equatorial arc patterns were formed as the PVA crystal-

lites aligned in the drawing direction (see, e.g., Figs. 6 (b) and (c)). Equation (1) was used to calculate the PVA crystal orientation factors based on the azimuthal intensity distributions for the PVA ($10\bar{1}$) reflection at a 2θ angle of 19.4 (see Table 3). Adding 0.5 wt% NFC enhanced the orientation factor, and greatly improved ultimate tensile strength and strain-at-break. Figures 6 (a), (b), and (c).

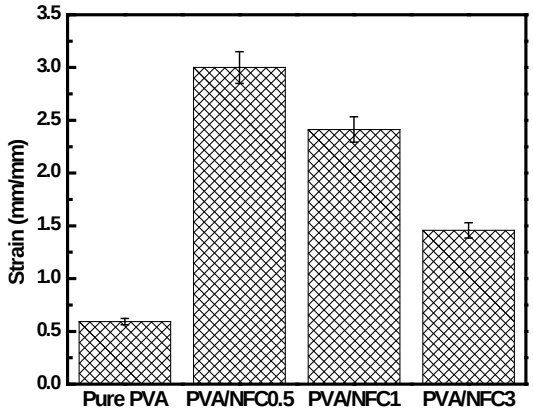

Figure 5. Strain-at-break of pure PVA and PVA/NFC filaments with different NFC contents.

Blade-cut cross-sections and side surfaces of the filaments were examined using SEM. As shown in Fig. 7, the diameters of the circular cross sections of the PVA/NFC filaments were about 90 to 110 μm after eliminating the side flash induced by blade cutting. The diameter value was similar to that based on the filament cross-section area calculations (cf. Table 2). Due to formation of a skin layer, followed by significant shrinkage during preparation, the side surfaces of the filaments show pleats. Also, NFC could not be found in cross section SEM images even at large magnification.

Table 3. PVA crystal orientation factors for PVA/NFC filaments with a draw ratio of 5.

Filament Samples	π, PVA Crystal Orientation Factor
Pure PVA	0.872
PVA/NFC0.5	0.923
PVA/NFC1	0.915
PVA/NFC2	0.913
PVA/NFC3	0.908

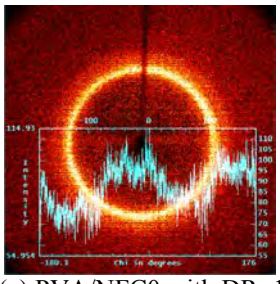
(a) PVA/NFC0 with DR=1

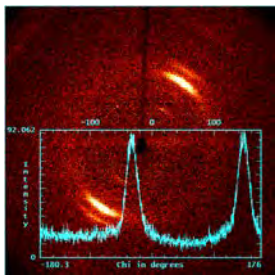
(b) PVA/NFC0 with DR=5

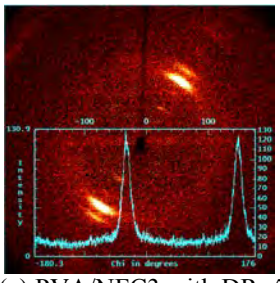
(c) PVA/NFC3 with DR=5

Figure 6. X-ray diffractograms of pure PVA and PVA/NFC filaments, and azimuthal intensity distributions for the ($10\bar{1}$) PVOH reflection, for (a) pure non-stretched PVA, (b) stretched pure PVA, and (c) stretched PVA/NFC3. The numbers 0 and 3 refer to the NFC content, and DR denotes the draw ratio.

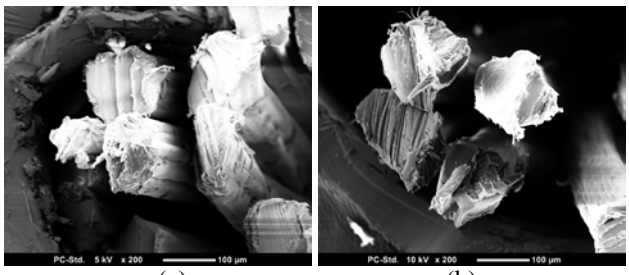
(a) (b)

Figure 7. SEM images of the surface structures of blade-cut PVA/NFC05 and PVA/NFC3 filaments in the cross-section direction. The white scale bar denotes 100 μm.

In the PVA/NFC solution preparation process, high shear stress was beneficial in helping disperse NFC in the viscous PVA solution. Nonetheless, high shear stress also resulted in a reduction in the PVA solution's viscosity, probably due to a reduction in the PVA's molecular weight (i.e., material degradation). To investigate the

degradation effects, viscosity differences of various pure PVA solutions prepared under different processing conditions were measured and are listed in Table 4. In Fig. 8, PVA solution viscosities via different processing conditions exhibited varying viscosity reductions compared with the pure PVA solution. According to the experimental design, the number of passes and the microchamber pressure difference were the first and second most important parameters causing a reduction in viscosity, suggesting molecular weight degradation.

Table 4. Various processing parameters used to investigate high shear on PVA molecular weight reduction.

Sample #	% PVOH in solution	Chambers used (μm)	Number of passes	Pressure* (psi)
0	13	n/a	n/a	n/a
1	13	87	1	Low
2	13	87	1	High
3	13	87	3	Low
4	13	87	3	High
5	13	200/87	1	Low
6	13	200/87	1	High
7	13	200/87	3	Low
8	13	200/87	3	High
Note: All specimens that were run through the microfluidizer were heated to 70C				
*Pressure set pts: Low = 10,000 psi; High = 28,000 psi				

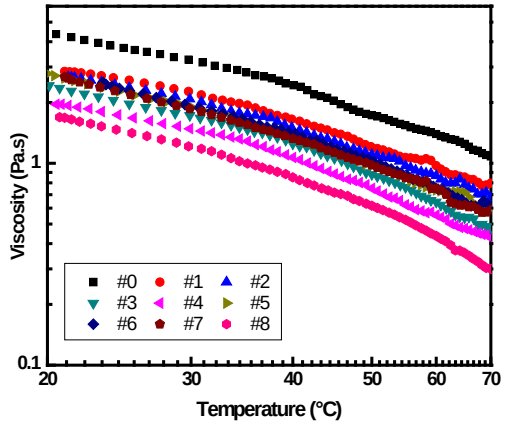

Figure 8. PVA solution viscosities corresponding to various processing conditions with respect to temperature.

Conclusions

This paper presents a new four-step process to fabricate continuous PVA/NFC filaments with a draw ratio of 5. Compared to undrawn neat PVA filaments, the stretched PVA/NFC nanocomposite filaments exhibited noticeably improved mechanical properties (i.e., ultimate tensile strength, Young's modulus, and strain-at-break). Furthermore, PVA/NFC3 had the highest ultimate tensile strength at 396 MPa. To achieve good NFC dispersion in viscous PVA solutions, high shear is beneficial to disperse the NFC fibers. However, strong shear stress likely also reduces the PVA's molecular weight (i.e., material degradation) as reflected by the reduction in solution viscosity. The number of passes the PVA/NFC solution makes through the microfluidizer and the chamber pressure difference are the processing parameters that cause the greatest reduction in the viscosity. Further work needs to be performed to find the appropriate processing that results in good NFC dispersion but limits molecular weight reduction.

Acknowledgements

The authors would like to acknowledge the financial support of the USDA National Institute of Food and Agriculture Award (No. 2011-67009-20056) and the Wisconsin Institute for Discovery at UW–Madison. The first author also wishes to acknowledge the National Nature Science Foundation of China (No. 51073601, No.21174044), the Fundamental Research Funds for the Central Universities (No.2011ZZ0011), the China Postdoctoral Science Foundation (2012M511791), and the 973 Program (2012CB025902) for their financial support.

References

1 R. J. Moon, A. Martini, J. Nairn, J. Simonsen and J. Youngblood, Chem. Soc. Rev., 40, 3941 (2011).
2 S. Iwamoto, A. N. Nakagaito, and H. Yano, Appl. Phys. A: Mater. Sci. Process., 2007, 89, 461-466
3 T. Zimmermann, N. Bordeanu and E. Strub, Carbohydr. Polym., 79, 1086 (2010).
4 A. Dufresne, J. Y. Cavaille and M. R. Vignon, J. Appl. Polym. Sci., 64, 1185 (1997).
5 R. K. Johnson, A. Zink-Sharp, S. H. Renneckar and W. G. Glasser, Cellulose, 16, 227 (2009).
6 S. Iwamoto, A. Isogai, and T. Iwata, BioMacromol, 12, 831 (2011).
7 A. Walther, J. Timonen, I. Diez, A. Laukkanen, and O. Ikkala, Adv. Mater. 23, 2924 (2011).
8 H. Sehaqui, N. Mushi, S. Morimune, M. Salajkova, T. Nishino and L. Berlund, ACS Applied Materials and Interfaces, 4, 1043 (2012).
9 M. Nishiyama, Chem. Fibers Int. 47, 296 (1997).
10 K. Wong, M. Allmang, L. Hutter, H. Luong, W. Wan, Carbon 47, 2571 (2009).
11 M. Ji, W. Lee, R. Karim, and et al., Colloid Polym. Sci, 287, 751 (2009).
12 V. Favier, G. Canova, J. Cavaille, H. Chanzy, A. Dufresne, Polym. Adv. Technol. 6, 351 (1995).
13 A.Uddin, J. Araki, and Y. Gotoh, BioMacromol, 617, 12 (2011).
14 M. Peresin, Y. Habibi, J. Zoppe, J. Pawlak and O. Rojas, ioMacromol, 11, 674 (2010).
15 T. Saito, S. Kimura, Y. Nishiyama, and A. Isogai, BioMacromol, 2485, 8 (2007).

Keywords: NFC, PVA, nanocomposites, filaments, tensile properties